Astroparticle Physics 132 (2021) 102615

Contents lists available at ScienceDirect

Astroparticle Physics

journal homepage: www.elsevier.com/locate/astropartphys

Electrical structure of the thundercloud and operation of the electron accelerator inside it

A. Chilingarian [a,b], G. Hovsepyan [a], E. Svechnikova [c], M. Zazyan [a]

[a] A. Alikhanyan National Lab (Yerevan Physics Institute), Yerevan 0036, Armenia
[b] National Research Nuclear University MEPhI, Moscow 115409, Russia
[c] Institute of Applied Physics of RAS - 46 Ul'yanov str., 603950, Nizhny Novgorod, Russia

ARTICLE INFO

Keywords:
TGE
RREA
Atmospheric electricity
Particle detectors

ABSTRACT

The most powerful particle accelerators operating in thunderclouds send in direction of the earth's millions and millions of electrons, gamma rays, and rarely neutrons. The emerging electrical structures in the atmosphere which make it possible to accelerate seed electrons from an ambient population of cosmic rays up to ≈70 MeV are still an area of intensive research. We discuss the main scenarios of the thundercloud charge structure supporting the emergence of an electric field strong enough to help electrons run away and create electron avalanches (RREA). After coming out of the accelerating electric field in the thundercloud, the RRE avalanche significantly attenuates and reaching the earth's surface is measured by the particle detectors and spectrometers as thunderstorm ground enhancement (TGE). Energy spectra of the measured fluxes of electrons and gamma rays can be used to reveal the charge structures giving rise to RREA. We perform simulation of the RREA development in the thundercloud with CORSIKA code and compare energy spectra of RREA corresponding to different configurations of the intracloud electric field with energy spectra of TGE measured in summer 2020. We invoke also additional evidence, namely the hydrometeor density profiles obtained with the weather research and forecast model (WRF) to confirm disclosed charge structures.

1. Introduction

The atmospheric electric fields and atmospheric discharges were intensively investigated in the last decades using radars, 3D lightning mapping arrays (LMA), worldwide lightning location networks (for instance WWLLN), and VHF interferometer systems, with synchronous measurements of near-surface electric field disturbances. The new messengers detailing information on the atmospheric electric field are different species of cosmic rays, which include electrons, muons, gamma rays, and neutrons (comprising thunderstorm ground enhancements - TGEs [14]) registered on the Earth's surface by networks of elementary particle detectors.

Thunderclouds give rise to TGEs, which discloses the structure and strength of atmospheric electric fields. The origin of TGE is the relativistic runaway electron avalanche (RREA) developed in the terrestrial atmosphere when the strength of the electric field exceeds a threshold value, which depends on the density of the atmosphere [18].

Experiments completed during 1945–1948 at the Zugspitze Observatory in Germany [21] revealed a rather complicated structure of the intracloud electric field. Joachim Kuettner discovered a pocket of positive charge (Lower positive charge region - LPCR) in the base of the cloud and introduced the term "Graupel dipole" referring to the charge structure formed by LPCR and the main negatively charged layer. The localization of charged layers in the thundercloud can be rather sophisticated (see [25,26]), however, the tripole structure is assumed to be a basic configuration. The three-charge layer arrangement with 2 main charged regions (positive above negative) and - relatively small lower positively charged region (LPCR) is referred to as the classic tripole. Tsuchiya [27] suggested that during winter thunderstorms in Japan short-lived tripole structures appeared in a thundercloud. Eleven TGEs (authors call it gamma -glows) were registered in Japan during the last years [28]. Chilingarian and Mkrtchyan [6] discovered the major role of LPCR in TGE initiation and made the first classification of scenarios of TGE initiation based on the shape of the near-surface electric field disturbances. The charge structure of a thundercloud is depicted in Fig. 1. On the left side of the cartoon, we present electron avalanches developed in the lower dipole (TGE) and upper dipole of the thundercloud (so-called terrestrial gamma flashes, TGFs, [17]). Red arrows denote 3 electric fields: downward directed field in the upper dipole of the cloud formed by the main negative (MN) and upper positive charge, the upward-directed field in the lower dipole formed by MN and the LPCR, and upward-directed field formed by MN and its mirror (MIRR) image in the ground. Throughout this paper, we use the atmospheric electricity sign convention, according to which the downward directed electric

https://doi.org/10.1016/j.astropartphys.2021.102615
Received 2 March 2021; Received in revised form 3 May 2021; Accepted 28 May 2021
Available online 3 June 2021

field or field change vector is considered to be positive. Thus, the negative field measured by the EFM-100 electric field mill corresponds to the dominant negative charge overhead (upward-directed electric field).

The RREA is a threshold process, which occurred only if the electric field exceeds the critical value in a region of the vertical extent of about 1–2 km. The threshold (critical) energy smoothly increases with the increase of air density according to $E_{th} = n \bullet 2.84$ kV/cm [2,16], where n is the relative air density, i.e., the relative density normalized to the sea level value, that equals to 1.225 kg/m^3.

Following possible scenarios of electron acceleration in the atmospheric electric fields can be considered:

1 The dipole formed by MN and its mirror image at the ground (hereafter, MN-MIRR) that accelerates electrons downward. If MN charge is very large inducing a very strong electric field that exceeds the critical value, the RREA can be unleashed and TGE will be large, and energies up to 50 MeV will be observed. The near-surface electric field is deep negative reaching TGEs −30 kV/m for the largest TGEs. Thus, regardless of the cloud base location, the electric field extends almost down to the earth's surface, and both gamma rays and electrons can be registered by particle detectors and spectrometers.
2 When/if LPCR emerged, additionally to the MN-MIRR, another dipole is formed by MN-LPCR. For few minutes, when LPCR is mature and screens the detector site from the negative charge of MN, the near-surface field is in the positive domain. TGE can be very intense in Spring when LPCR is very close to the earth's surface (25–50 m, [9]). Fields induced by the MN-mirror and MN-LPCR are identically directed and their sum can reach rather large values exceeding the threshold value to start RREA by 20–30%. In Summer, the distance to the cloud base is larger (200–400 m) and usually only gamma rays reach the earth's surface and are registered by the particle detectors. Electrons are attenuated in the dense atmosphere. In Autumn, again LPCR can be low and electric filed in the cloud very large unleashing strong prolonged RREAs and, consequently, gigantic TGEs.

In addition to these basic scenarios, the fast-changing charge structure of the cloud produces a more complicated configuration of the electric field. For instance, TGE can start with mature LPCR, but after its contraction, only MN-MIRR sustains a strong electric field. Alternatively, in the middle stage of the first scenario, the LPCR is formed and for a few minutes, the near-surface electric field rises and reaches positive values, and then returns again to deep negative values when LPCR is depleted.

Lightning flashes reduce the negative charge above the earth's surface, thus decreasing the electric field in the lower dipole below the RREA threshold. RREA declines and high energy particles are eliminated from the TGE flux. However, a smaller near-surface electric field is still in place and 222Rn progeny continues to enhance the "background"

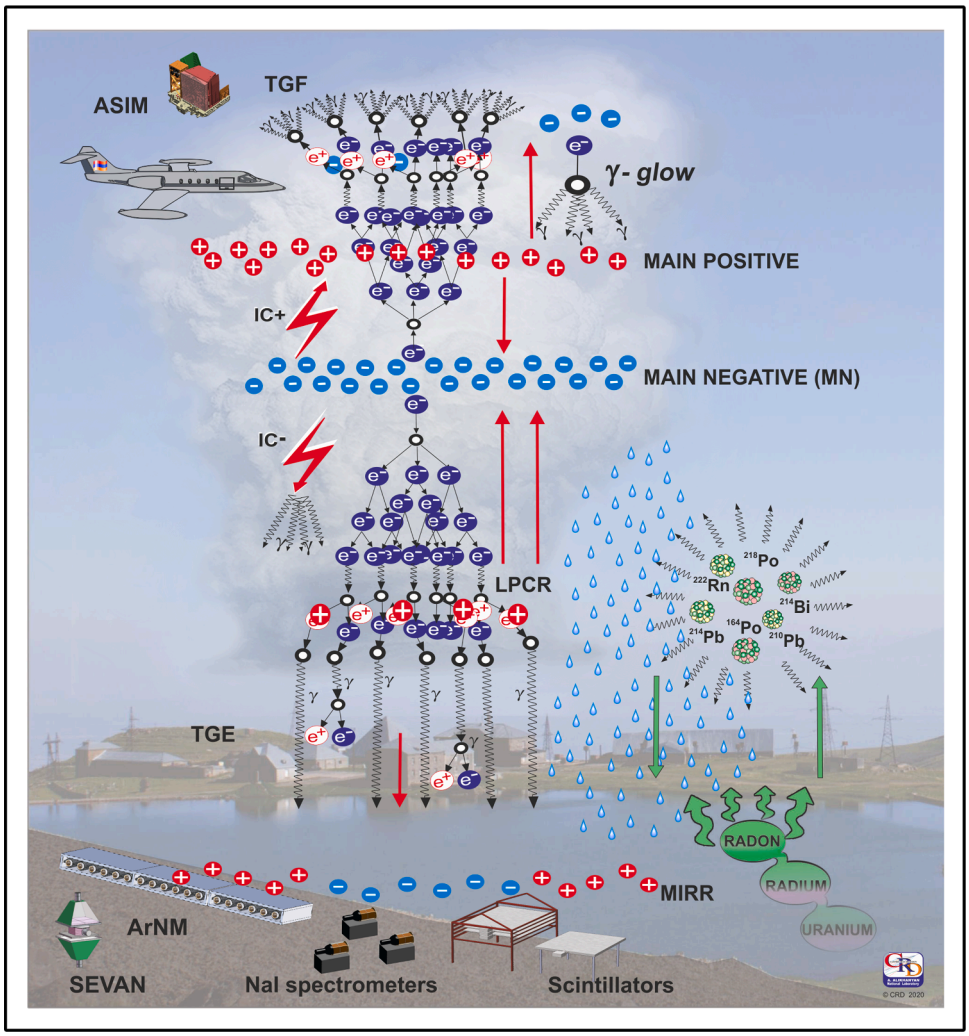

Fig. 1. The electrical structure and particle fluxes related to the thunderstorm. Particle flux initiation in thundercloud (RREA) on the left side, Rn222 progeny radiation on the right side.

gamma ray flux, initiating long-lasting TGE [10]. TGE continues also after the returning of the near-surface electric field strength to the fair-weather value due to tens of minutes long life-time of 214 Pb and 214Bi. The rain brings back the Rn222 progeny from the atmosphere to the earth's surface and for several tens of minutes provides additional gamma ray radiation (the washout effect, see [13]). Thus, the scenarios of the origination of the downward electron-accelerating electric field are numerous and the corresponding TGEs may vary in intensity and energy spectra; corresponding near-surface electric field also can exhibit several reversals.

In 2009–2020, the Aragats facilities registered more than 500 TGEs (see the first and second catalogs of TGE events in [7,9]). Numerous particle detectors and field meters are located in three experimental halls as well as outdoors; the facilities are operated all year round providing continuous registration of the time series of charged and neutral particle fluxes on different time scales and energy thresholds. In this paper, we present precise measurements of the electron and gamma ray energy spectra made by the large scintillation spectrometer along with detailed simulations with CORSIKA code of the RREA process in the electrified atmosphere. We demonstrate that RRE avalanche simulation with realistic strengths of the electric field yields particle fluxes quite compatible with the measured ones, thus, proving the validity of the RREA origin of the TGE phenomenon. Also, we present and discuss structures of the atmospheric electric field for interesting TGEs observed in 2020, during which we observe several scenarios of the cloud electric structure.

To confirm the electric field structures obtained with modulated particle fluxes, additional evidence on the hydrometeor density distribution density in the thundercloud obtained from the numerical modeling of the state of the atmosphere was used. Weather research and forecasting model (WRF, https://www.mmm.ucar.edu/weather-research-and-forecasting-model) is widely used in research applications, providing information on the structure and dynamics of all types of convective systems with a horizontal resolution of about 1 km, which is difficult to attain with other methods. Thus, we made an initial step on the way to a detailed investigation of the structure of TGE-producing clouds. We will test if the WRF model can confirm the "large-scale" structure of the cloud obtained by the "screening" of the cloud with "beams" of electrons and gamma rays.

2. Energy spectra analysis of RREA electrons and gamma rays

Measurement of the energy spectrum of RREA electrons is a rather difficult problem. After exiting the region of a strong electric field where electrons are accelerated and multiplied, the intensity of the electron beam rapidly declines due to ionization losses. On the other hand, gamma rays are attenuated much slower; thus, at the earth's surface, after propagation over a few hundreds of meters the intensity of gamma rays is 20–30 times larger than the intensity of electrons (if any).

NaI spectrometers, with a very small area (usually 0.01–0.03 m^2) measure usually only gamma ray flux, and, sometimes, where TGE is extremely intense also a small fraction of electrons. Therefore, at present the only spectrometer capable of registering RREA electrons and recover their energy spectrum is the ASNT detector located at Mt. Aragats, see details in [8]. The detector consists of a 4 m^2 and 60 cm thick plastic scintillator (more than 100 times bigger than the largest NaI crystal used in atmospheric high-energy physics measurements) and has the capability to separate charged and neutral particles. From the ASNT detector, we obtained a 2-second time-series of count rate and 20-second time series of histograms of energy releases in a 60-cm thick plastic scintillator. After performing a full GEANT4 [1] simulation of the detector response function we recover differential and integral energy spectra of RREA electrons and gamma rays. Three TGEs observed in 2020 were selected for the analysis presented in this study. These TGE events occurred in different conditions of the atmospheric electric field, declined naturally, or terminated by the lightning flashes. On 27 June 2020, a large storm lasting 2.5 h occurred on Aragats. Attempts to start TGE began at 19:01, 19:06, and 19:07; all were terminated by lightning flashes shown by red arrows in Fig. 2a. TGE started at 19:08 characterized by a long duration (≈20 min) with near-surface electric field in the negative domain during the maximum of the TGE flux and with field reversals at the decaying stage of TGE, see Fig. 2a. We suppose that the TGE start at 19:08–19:11 was controlled by the mature LPCR that produced a positive near-surface electric field. The height of the cloud estimated from the outside temperature and the dew point was ≈150 m.

After the near-surface field polarity reversal from positive to negative at 19:11, the atmospheric electric field was controlled by the main negative charge region only, and during 7 min the field strength remained below −20 kV/m. During this time interval, the particle flux continued to rise above the background reaching 15% enhancement above the background. At 19:18 another near-surface electric field polarity reversal from negative to positive occurred and the near-surface electric field was controlled again by a newly formed LPCR. As a result, the field strength remained ≈15 kV/m for 10 min. During this minute's particle flux slowly decayed, staying constant for a few minutes, and finally terminated at 19:31.

On July 23 the TGE started at 20:04 when near-surface field was in the negative domain (−10 kV/m) and start to fast rise at 20:07 when the electric field decreases to −14 kV/m (Fig 2b). At 20:09–20:11, a short outburst to positive domain occurred (+6 kV/m) evidencing an LPCR emergence, which coincides with the maximum of the TGE flux (16%), that was twice larger comparing with the maximum flux of the TGE described above (Fig. 2a). According to the second main scenario of TGE initiation this 3 min the intracloud electric field MN-MIRR was intensified by the emerging MN-LPCR field and RREA strengthened by the enlarged field. The TGE that occurred on 14 June 2020 will be analyzed in more detail in the last section of the paper.

In Fig. 3a and b, we present differential energy spectra of these two TGE events for the minute of the highest flux (power-law fit I (E) = $A{\cdot}E^{-\gamma}$). Three histograms (20 s each) collected by ASNT detector were joint to form a 1-minute histogram of the energy releases in a 60 cm thick scintillator for the further recovering of the energy spectra using the response function of spectrometer obtained with GEANT 4 simulation.

In Table 1 we show summer TGE intensities (integral spectra above 4 MeV) and spectral indices of the differential energy spectra, as well as maximum energies of electron and gamma ray fluxes. For the reader convenience in the last rows of Table 1 we show also analogical parameters of the simulated events to be discussed in the next section. Intensities of the electron fluxes are much lower comparing with gamma ray fluxes, the maximum energies of the gamma ray flux are larger than the electron ones as well. Thus, the measured parameters of the TGE particle energy spectra show that the TGE particles leave the strong (accelerating) electric field considerably high on 150–200 m above particle detectors (usual for the summer TGEs). These numbers are in agreement with the approximate estimation of the cloud base height. However, the cloud base height is not mandatory coincides with the electric field termination, especially for the 1 scenario (only NM-MIRR dipole). We will continue the discussion on the energy spectra of the TGE and RREA particles in the following sections.

3. CORSIKA simulations of the RREA process above ARAGATS station

To understand the avalanche development in the electrified atmosphere and to compare measured energy spectra with simulated ones we used the CORSIKA code [19] version 7.7400, which takes into account the effect of the electric field on the transport of particles [3]. As was already demonstrated by GEANT4 and CORSIKA simulations [5,12], the RREA process is a threshold process and avalanches can be started when the atmospheric electric field exceeds the threshold value that depends on the air density. The extent of the electric field also should be

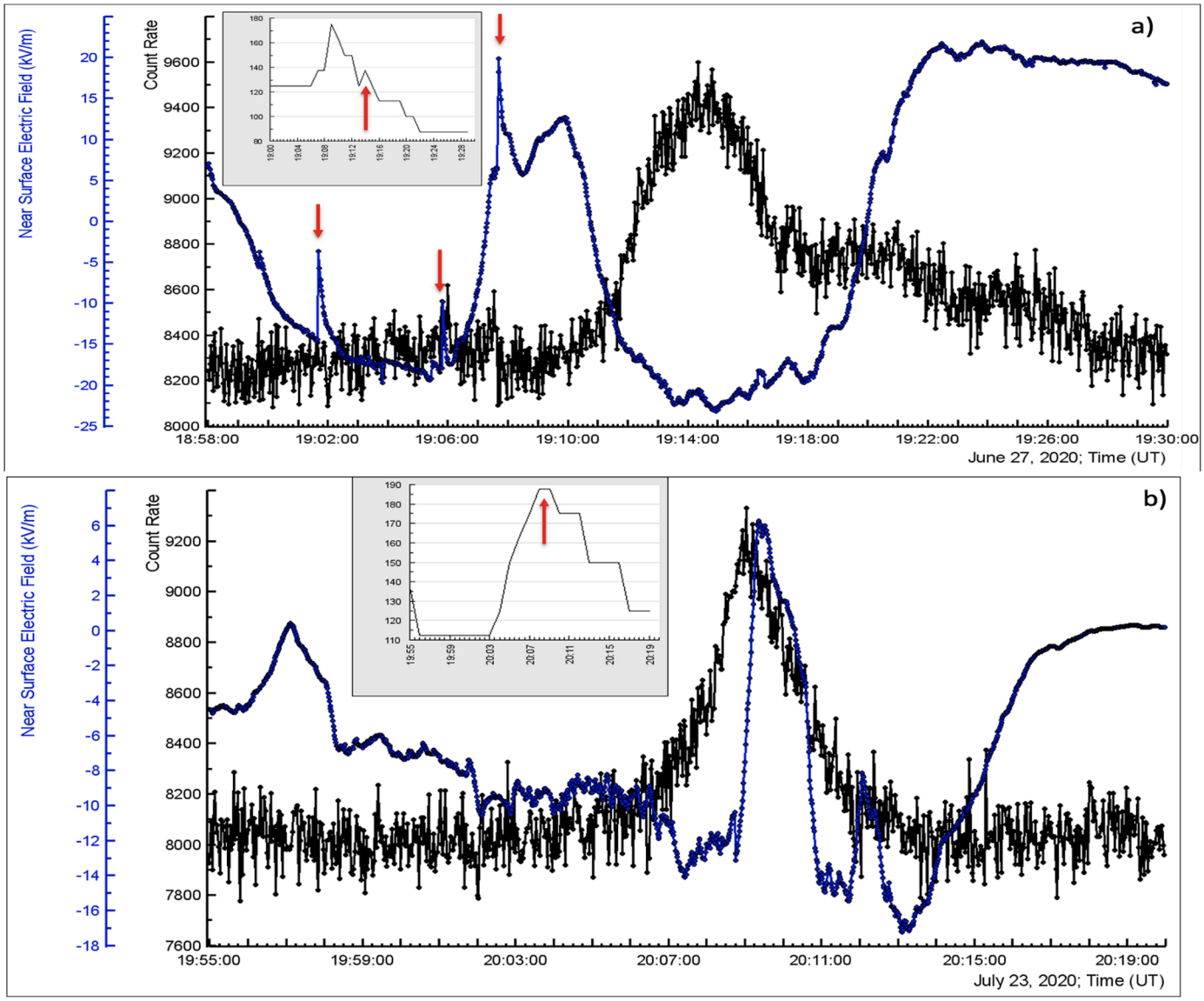

Fig. 2. The time series of count rate measured by a 60-cm thick scintillator (black) and disturbances of the near-surface electric field (blue). In insets we show the evolution of cloud base height during TGE development. By red arrows, lightning flashes that stopped attempts to start TGE and the approximate heights of the cloud base during TGE are shown.

sufficiently large to ensure avalanche development. The development of RREA will certainly increase the electrical conductivity in the cloud. In numerous studies [22,24] was shown that lightning flash occurs after the RREA initialization threshold exceeds 10–40%. The RREA simulation codes do not include the lightning initialization mechanism, thus one can exceed the strength of the electric field above any reliable value to get billions and billions of avalanche particles, but it is not physically justified. Thus, we do not test electrical fields stronger than 2.2 kV/m and weaker than 1.8 kV/cm (at the heights 3–6 km a.s.l.). The simulation of the RREA was done within the vertical region of the uniform electric field with strengths exceeding the runaway breakdown threshold by a few tens of percent on height 5400 m. The assumed uniformity of the electric field leads to the change of the surplus to the critical energy at different heights corresponding to the particular air density. The energy spectrum of seed electrons was adopted from the EXPACS WEB calculator [23] following the power low with power index - 1.173 in the energy range 1–300 MeV. The number of seed electrons from the ambient population of secondary cosmic rays was obtained from the same calculator, to be 42,000 with energies above 1 MeV. The estimated distance to the cloud base during large TGE is usually 25 – 200 m (see Fig 17 in [11]), thus in our simulations, the particle avalanches continued propagation in the dense air additionally 25, 50, 100, and 200 m before registration. Simulation trials include from 10^3 to 10^4 events for the electric field strengths of 1.8–2.2 kV/cm. The propagation of electrons and gamma rays were followed in the avalanche until their energy decreased down to 0.05 MeV.

CORSIKA code follows the development of the RREA and calculates the number of electrons and gamma rays in RREA on different stages of avalanche development in the strong electric field and after leaving it additionally 200 m. Corresponding energy spectra for 3400 and 3200 m height are posted in Fig. 4. In Fig. 4a we can see that at the exit from the electric field on 3400 m height the number of electrons exceeds the number of gamma rays, however, after propagating in 200 m of dense air on 3200 m height the electron flux rapidly attenuates (see Fig. 4b), the number of gamma rays does not significantly change. The maximum energies of electrons as well were larger at 3400 height, and smaller at 3200. The high-energies tail of gamma ray spectra shown in Fig. 4 is due to modification of the electron energy spectrum enhancing probability of bremsstrahlung radiation by high energy electrons (MOS effect, for details, see [5]).

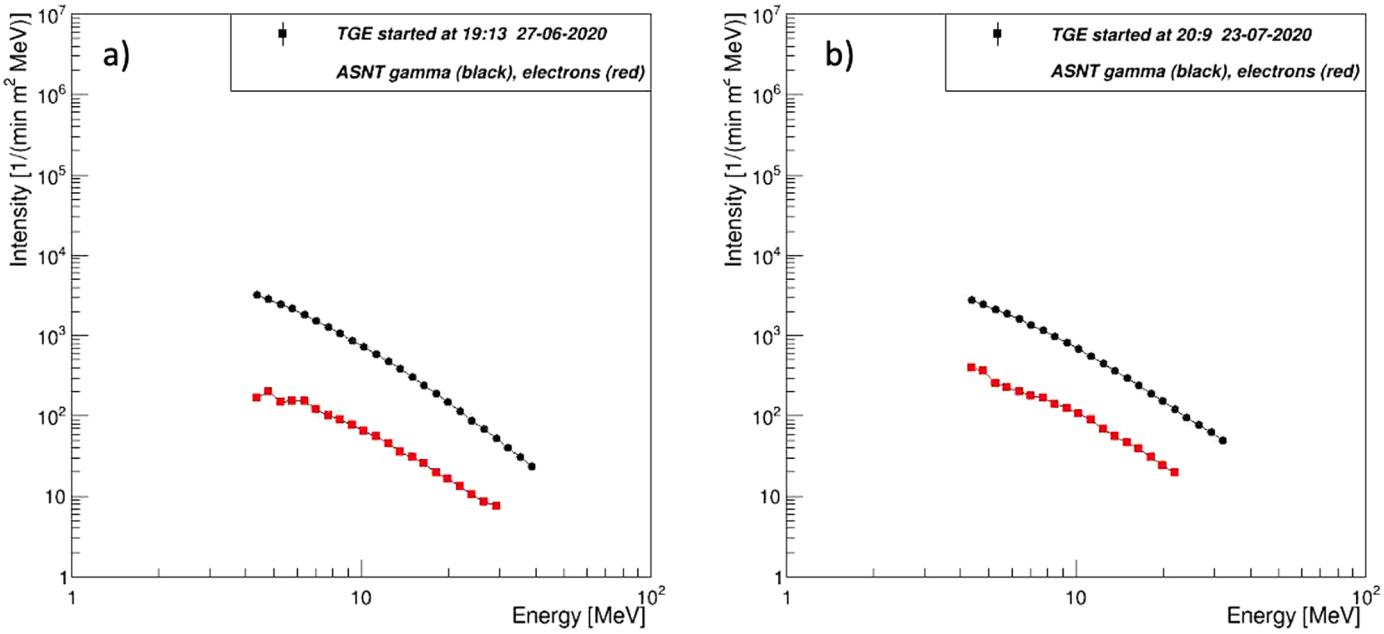

Fig. 3. Differential energy spectra of RREA electrons (red) and gamma rays (black) measured by ASNT spectrometer at altitude 3200 m at highest particle flux above 4 MeV.

Table 1
Parameters recovered from the ASNT spectrometer energy spectra and simulated with CORSIKA code energy spectra (power law fit I (E) = $A{\cdot}E^{-\gamma}$).

Date and Time	Integral spectra above 4 MeV (1/(m^2 min MeV)		Spectral indices (γ)		Maximum energy (MeV)	
	Electrons	Gamma rays	Electrons	Gamma rays	El.	Gamma rays
14/6/2020 19:41	6.02E+03	5.27E+04	2.45±0.08	2.89±0.01	20	39
27/6/2020 19:13	1.72E+03	2.13E+04	2.11±0.03	2.52±0.01	32	43
23/7/2020 20:09	2.48E+03	2.02E+04	1.91±0.02	2.16±0.01	24	35
1.9 kV/cm on 3200 m	2.86+03	1.33E+05	2.94±0.08	3.30±0.011	27	60
1.8 kV/cm on 3200 m	0.99+03	2.71E+04	1.82±0.12	2.64±0.016	22	50

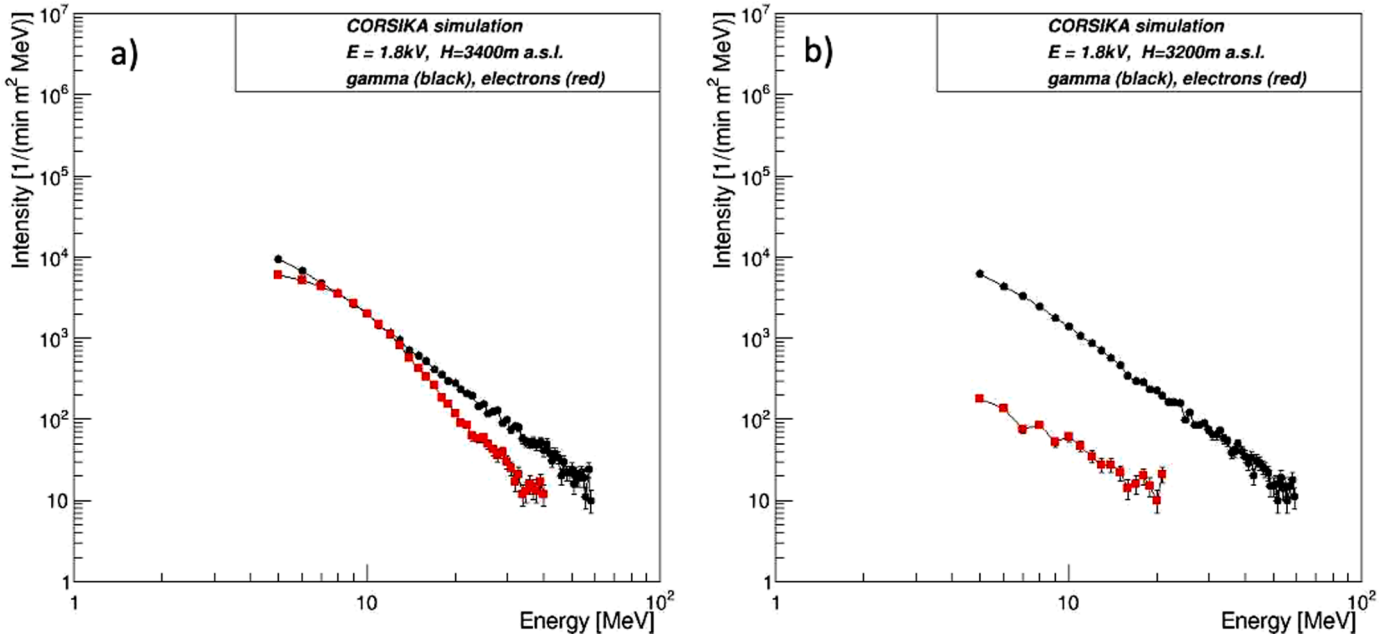

Fig. 4. Differential energy spectra of electrons and gamma rays at altitudes 3200 and 3400 m (just at exit from the intracloud electric field). 42,000 seed electrons were introduced in the electric field of 1.8 kV/cm strength at the height of 5400 m.

In Table 1 we compare parameters of electrons and gamma ray energy spectra of the modeled RREAs obtained with CORSIKA code (for 1.8 and 1.9 kV/m intracloud electric field) and measured TGEs. The main parameters of the experimental and simulated energy spectra also shown in Figs. 3 and 4b are close to each other and prove that the RREA process with selected parameters of the intracloud electric field can surely produce TGEs measured on Aragats and at other locations (on mountains Lomnicky Stit, Musala, etc.). The smoother shape of the experimental spectra is explained by the procedure of recovering energy spectra from the measured histograms of the energy releases in the spectrometer. The calculation of the energy response function, including propagation of particles through the detector, modeling of the bin-to-bin migration, and others introduce smoothing of recovered energy spectra (see for details in [20]). For the simulated spectra, we do not include the detector response function calculation.

In Fig. 5 we show the development of the RRE avalanches at different depths in the atmosphere and for various physically justified strengths of the intracloud electric field. The curves are recalculated to one seed electron for easier comparison with experimentally measured intensities. The numerical data corresponding to Fig. 5 is posted in Table 2. For the lower electric field strengths (1.8 and 1.9 kV/cm) the RREA process attenuates before reaching the observation level at 3200 m (see green and brown curves in Fig. 5a), as the critical value on the height ≈ 4000 m is ≈1.9 kV/cm. Thus, for the not very large TGE events (the ones measured in the summer 2020 and shown in Fig. 3), the extent of the accelerating electric field is less than 1500 m and a potential drop in the cloud - less than 250 MV.

Normalizing numbers of electrons and gamma rays obtain in simulation trials and in TGE measurements by the number of trials and by the number of seed electrons on 5400 height correspondingly we can select plausible parameters of the RREA that can produce TGEs registered in summer 2020, see Table 2 and Fig. 5 (the blue line corresponds to the TGE occurred on 14 June). In the first 2 columns of Table 2 we post the parameters of the intracloud electric field used in the simulations and the date of TGE. The number of electrons and gamma rays per seed electron for different electric field strengths and termination heights, as well as experimentally measured intensities, are shown in the third and fourth columns. From Table 2 and Fig. 5 we can see that the number of electrons and gamma rays per seed electron of relatively small TGEs occurred in 2020 more-or-less satisfactory match Monte Carlo calculations of the RREA developing in the electric field of 1.8 - 1.9 kV/cm strength, which ends 100–200 m above earth's surface. For the RRREA in the field of 2.0 kV/cm, the obtained number of gamma rays per seed electron (22) highly exceeds the measured in 3 TGE events values.

Sure, we cannot expect precise coincidence due to very specific atmospheric conditions for every measured TGE and several assumptions in simulations, which are more or less arbitrary. We assume a 2000 m extend of the electric field (however for the electric field 1.8 kV/cm the electron acceleration was possible only in 1000 m if RREA started on 5400 m). From the recent analysis of one of the TGEs measured on Aragats in 2017 the authors of [26] derive a much shorter extend of the electric field (300 m). We do not consider the contribution of the seed electrons with energies less than 1 MeV; we neglect also the impact of positrons. Nonetheless, from the simulations, we can conclude that the RREA process in the thundercloud within the parameters used can satisfactorily explain the TGE phenomena. In the next section, we will consider the atmospheric conditions that support the TGE initiation.

Table 2
Parameters of the RREAs calculated with CORSIKA code and of 2 TGEs observed in 2020.

	Height of termination of el. field above detectors	N of el. $E>4$ MeV per seed electron	N of γ rays $E>4$ MeV per seed electron
1.8 kV/cm	100	0.03	0.78
1.9 kV/cm	100	0.12	3.9
1.9 kV/cm	200	0.08	3.1
2.0 kV/m	200	0.43	22
14/6/2020	–	0.14	1.26
27/6/2020	–	0.041	0.51
23/7/2020	–	0.059	0.49

3. A very specific storm on 14 June 2020 with 3 TGE episodes supported by different electric field structures

A short storm of approximately 1.5 h duration occurred at the beginning of Summer on Aragats, which nonetheless exhibits 3 different structures of the intracloud electric field supporting TGE origination. In Fig. 6 and Table 3 we show overall characteristics of 3 episodes of the particle flux enhancement and corresponding values of the TGE significance (the peak "height" in the number of standard deviations from the fair-weather value), energy spectra, main meteorological parameters, as well as distances to nearby lightning flashes, measured by Aragats solar neutron telescope (ASNT), EFM-100 electric mill, and DAVIS automatic weather station.

In Fig. 7 and in Table 3 we can see that the TGE that occurred at

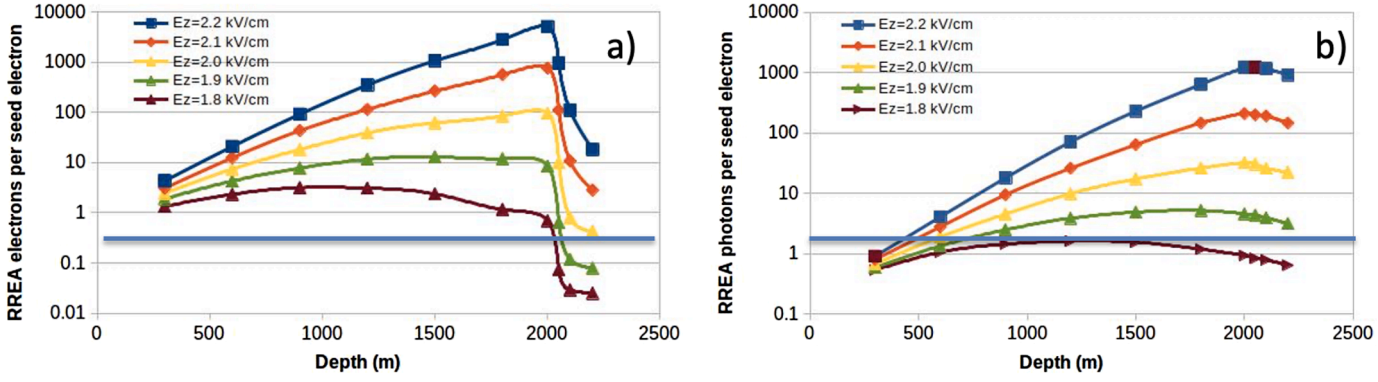

Fig. 5. Development of the RRE avalanche in the atmosphere. Avalanche started at 5400 m a.s.l. (0 depth), that is 2200 m above the Aragats station. The number of avalanche particles is calculated each 300 m. After exiting from the electric field propagation of avalanche particles is followed additionally 200 m before reaching the station. By blue line, we show the electron and gamma ray number per seed electron for the TGE that occurred on 14 June 2020.

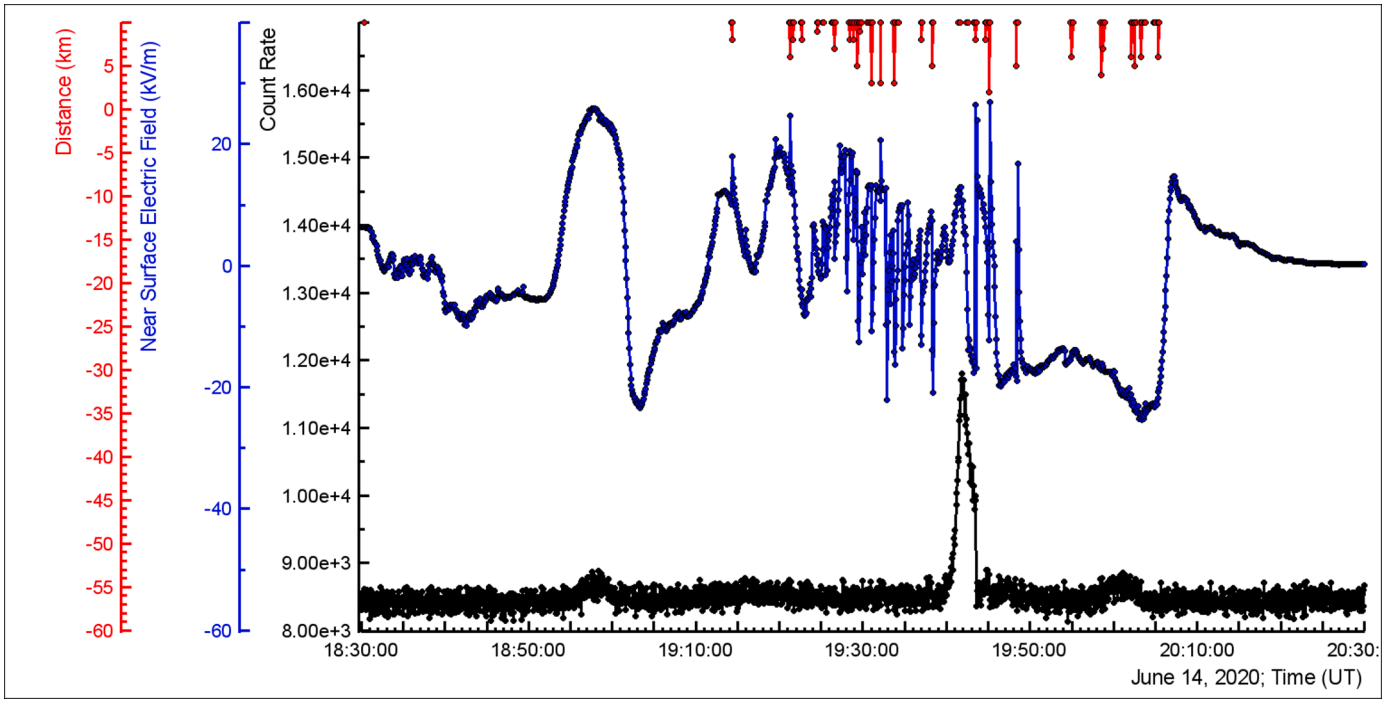

Fig. 6. At the bottom of the figure are depicted the time series of 2-sec count rates of ASNT (4 m^2 area, 60 cm thick scintillation spectrometer); in the middle – disturbances of the near-surface electric field measured by electric mill EFM-100 located on the roof of MAKET experimental hall; on the top red lines show the distance to nearby lightning flashed measured by the same electric mill (within 10 km distance only).

Table 3
Characteristics of 3 TGEs (peak significances, integral fluxes, maximum energies of electrons and gamma rays) and meteorological parameters measured and calculated for 3 episodes of particle flux enhancement on 14 June 2020.

	18:59 UT	19:42 UT	20:01 UT
Peak enhancement, 2-sec time series (%)	5.6	40	5
Peak enhancement, N of standard dev.	3	20	2.5
Electron flux >4 MeV ($1/m^2$min)	–	3000	–
Gamma ray flux > 4 MeV ($1/m^2$min)	2500	30,000	2000
Electron >4 MeV Max. energy (MeV)	–	20	9
Gamma ray > 4 MeV Max energy (MeV)	22	43	17
Temperature C°	4.7	2.8	1.7
Cloud height (m)	400	200	150
Atm. Pressure (mb)	693.7	693.8	694.2
Rel. humidity (%)	81	85	92

19:42 UT is the only one from 3 when electrons reach the earth surface; other2 smaller TGEs also are significant, demonstrating sizeable gamma ray flux at the minute of maximal enhancement, however, electron flux attenuates before reaching the earth's surface.

Maximum energies of gamma ray flux for all 3 events exceed 10 MeV. Only RREA developed in the atmosphere can accelerate seed electrons from the ambient population of cosmic rays to such large energies. The maximum energy of gamma ray flux exceeds the maximum energy of electrons more than 2 times, this indicates that the accelerating electric field is terminated high above particle detectors.

In Fig. 7c we show the zoomed version of the TGE that began at 18:57 UT. TGE occurred when the near-surface electric field was large and positive for several minutes (≈25 kV/m at a maximum of TGE). The distance to the cloud base was ≈400 m, see Table 3, thus the electron flux vanished before reaching the ground. The intensity of gamma ray flux reaches 2500 particles per m^2 per minute. RREA gamma ray flux on exit from the cloud was rather large not attenuated fully in the dense atmosphere. During the first TGE, no nearby lightning flashes were detected in the circle of 10 km and the near-surface field was changing rather smoothly.

In Fig. 7a and b we show the hydrometeor density distribution in the vertical plane simulated using the WRF model. The cloud is formed mainly by graupel- and snow-particles located on altitudes 0.5–2 km and 2–4 km above the Aragats station (3200 m) correspondingly. Measured near-surface electric field dynamics and large horizontal size of the "graupel" layer supports the assumption of the LPCR originated in the lower part of the cloud. The vertical extent of the electric field in the cloud can be 1–2 km, enough to allow the development of large electron-photon avalanches. Thus, the accelerating electric field is terminated high above the detectors, the electron flux declined and only gamma rays reach the earth's surface.

TGE which occurred half an hour later after numerous nearby inverted lightning flashes were supported by the mature LPCR and terminated by a -CG lightning, which occurred at 19:43:33.088, see Fig. 8c. The type of lightning was determined by the analysis of electric field changes measured in Aragats and Nor Amberd research stations (13 km apart). The polarity of electric field change was positive, and no polarity reversal of electric field change with distance has been detected, which indicates that a negative charge was destroyed in the cloud during the lightning flash [14,15]. The intensity of the particle flux was rather large. The integral spectrum of electrons at 3200 m was ≈3000 particles per m^2 per minute, and gamma rays – 30,000 per m^2 per minute for particles with energies above 4 MeV. For recovering energy spectra, we use a full simulation of the detector response function. Electron flux at the exit from the cloud at an altitude of ≈200 m has intensity 3 orders of magnitude larger than on earth's surface (obtained from simulations of RREA developed 2 km in the electric field of 1.8–2.2 kV/cm strength). The hydrometeor density distribution in the vertical plane presented in Figs 8a and 8b show a large-scale main negatively charged layer and lower positively charged layer. Thus, both MN-MIRR and MN-LPCR dipoles accelerate electrons downward.

In Fig. 9 we show the energy spectra of electrons and gamma rays

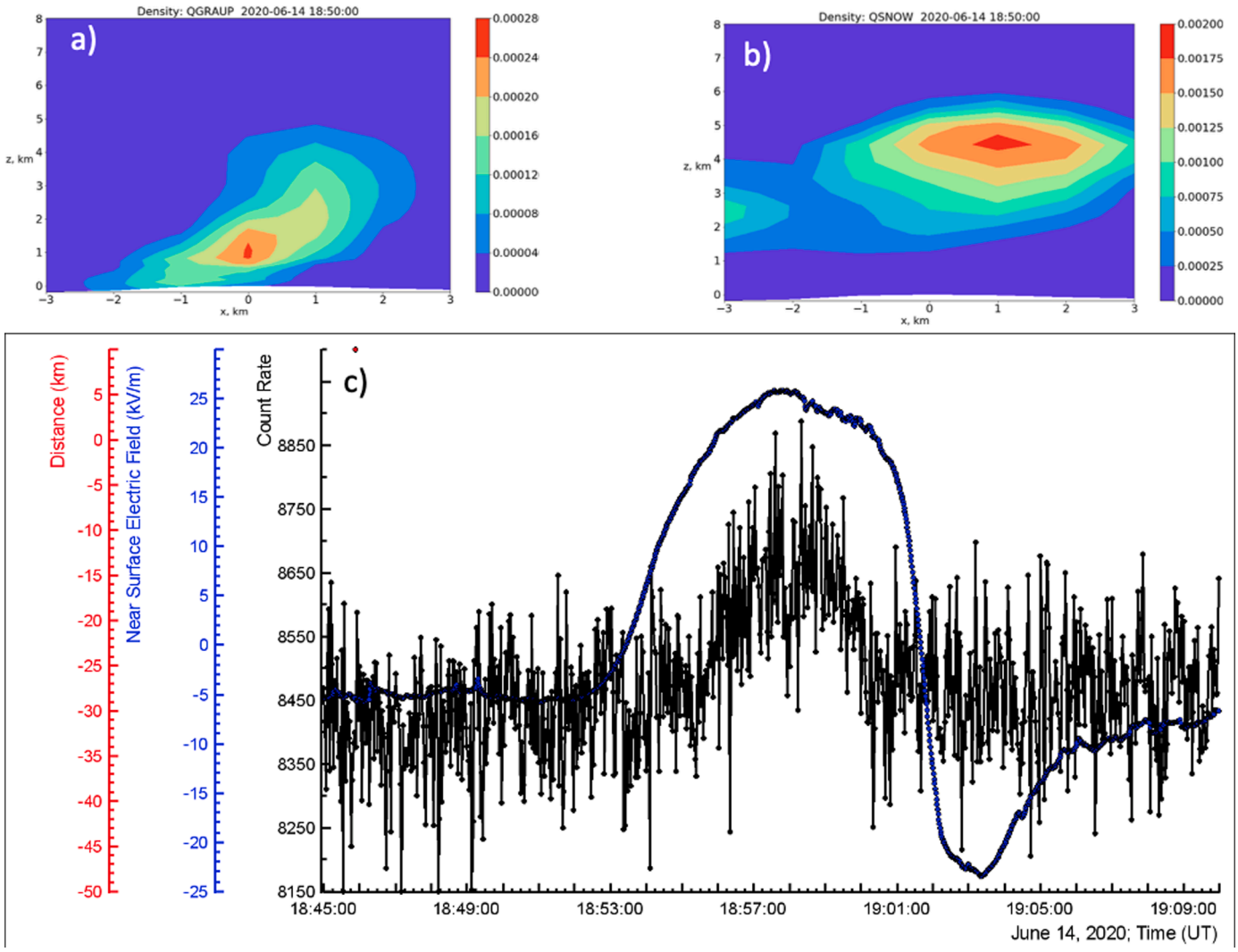

Fig. 7. In Fig. a) and b) we demonstrate the 2-dimensional patterns of the hydrometeor density (kg/m^3), according to the simulation using WRF. In Fig c) we show the zoomed version of the first TGE (the particle count rate measured by the ASNT detector and disturbances of the near-surface electric field measured by EFM-100 electric mill).

measured by the ASNT spectrometer on the earth's surface 3200 m. a.s.l. From the difference of the maximum energies of electrons and gamma rays, we can approximately estimate the height above detectors where the accelerated field was terminated. From simulations, we know that on the exit from the electric field the maximum energy of electrons is ≈20% higher than gamma rays. Thus, proceeding from the 39 MeV of gamma ray maximum energy we obtain ≈ 50MeV for the electron maximum energy. Therefore, energy losses of electrons in the atmosphere before reaching the spectrometer were 30 MeV, which corresponds to 150 m propagation in the air, if we assume the energy losses of the relativistic electron to be ≈200 keV/m. Sure, our calculation is approximate, giving mostly only the rough scale of cloud electric structure, however, if we assume the accuracy of LPCR localization not better than 50 m, our estimate is 80 m less than the cloud base estimate obtained by the meteorological method (230 m, using outside temperature and duw point, see inset in Fig. 9. As we mentioned above the cloud base height should not mandatorily coincide with the termination of the electric field, and we think that energy spectra analysis gives a reliable (although approximate) estimate of the height where the strong electric field terminates.

The third TGE that occurred around 20:00 was of the other type: the electron accelerating field was formed by the main negative layer only that produced the deep negative near-surface electric field on the Earth's surface, see Fig. 10d. No signs of LPCR are seen in the maps of the vertical profile of the cloud particles density, see Fig. 10a. The size of the main negative layer is rather small (compared with the one shown in Fig 8b when we have a much larger TGE) and correspondingly, the gamma ray flux was 15 times less than that for the TGE that occurred at 19:43 (Fig. 9b and Table 3). However, the maximum energy of gamma ray flux reaches 20 MeV and we can expect also the electrons to reach the earth's surface because in absence of the LPCR the electric field can extend down to the earth's surface. The answer to this contradiction we can find in Fig. 5a. Because the measured flux of TGE gamma rays is rather small, we can assume that the accelerating electric field was not very large. For the field strengths 1.8–1.9 kV/m the acceleration stopped at the depths 1000–1500 m (4400 – 3900 a.s.l.) Therefore, the declination of electron flux started far before they reach and exit the cloud base. Thus, it can be the reason for the absence of the TGE electron flux.

4. Conclusions

We measure the energy spectra of TGE electrons and gamma rays with a large scintillation spectrometer and estimate the maximum energies of both fluxes. We perform a cycle of simulations of the RREA process in the electric fields exceeding the runaway threshold by 10–30% and extended 2 km above particle detectors. In Figs. 4 and 5,

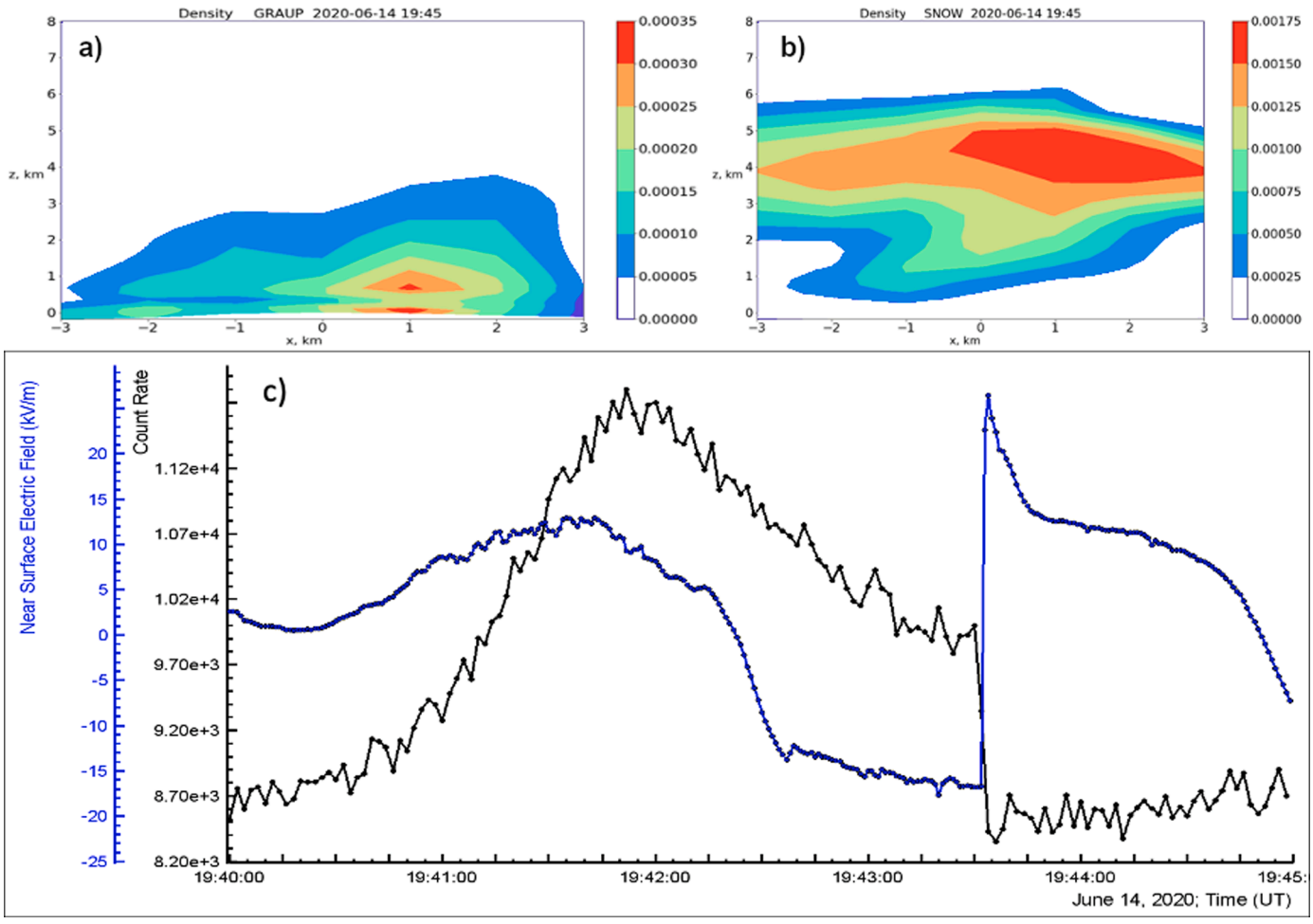

Fig. 8. a) and b) 2-dimensional patterns of the hydrometeor density (kg/m^3), according to the simulation using WRF. c) zoomed version of second TGE (the notion is the same as in Fig. 7).

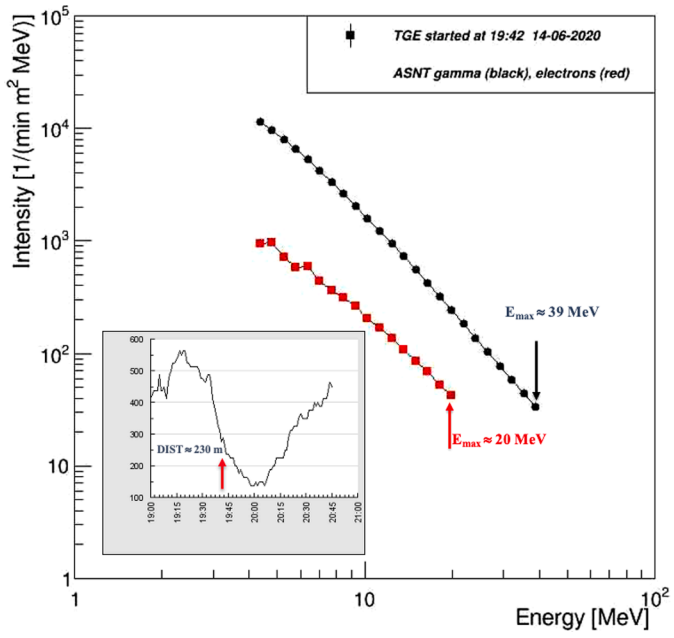

Fig. 9. Energy spectra of the electron and gamma ray content of TGE, by the arrows the maximal energies are denoted. In the inset, the distances to the cloud base are shown.

and Tables 1 and 2 we show that observed TGE events fit rather well to RREA simulations assuming 2 km field extension and 1.8–1.9 kV/cm electric field. Several plausible combinations of the intracloud electric field parameters initiated the RREA process, that can produce measured on Aragats TGEs. The number of RREA electrons (per one seed electron) abruptly decreases as avalanche exits from the region of the strong electric field. The sharp decrease of electrons after the exit from the electric field is confirmed in the experiment. The maximum energies of the simulated and observed spectra are in good agreement, and the relation between them obtained in simulations is confirmed by the observations as well.

A relatively few versions of field structure and strengths assumed in simulations are too small to reproduce the complicated and dynamic nature of the atmospheric electric field, in which particular RREA is developing to finally end up in a TGE. Nonetheless, the closeness of several measured and observed parameters allows us to confirm that the RREA is the origin of the TGE and to outline the most probable characteristics of the atmospheric electric field for particular observed TGE events. For fitting parameters of the particular TGE with appropriate RREA we need to solve the multiparametric optimization problem, including multiple solutions of the direct problem for finding plausible solution of the inverse problem [4].

We demonstrate 3 different configurations of the atmospheric electric field leading to the emergence of the RREA process and TGEs registered by the ASNT spectrometer. We explain the mechanisms of dipole origination and show how the emerged electrical structures in the atmosphere lead to the enhanced fluxes of electrons and gamma ray.

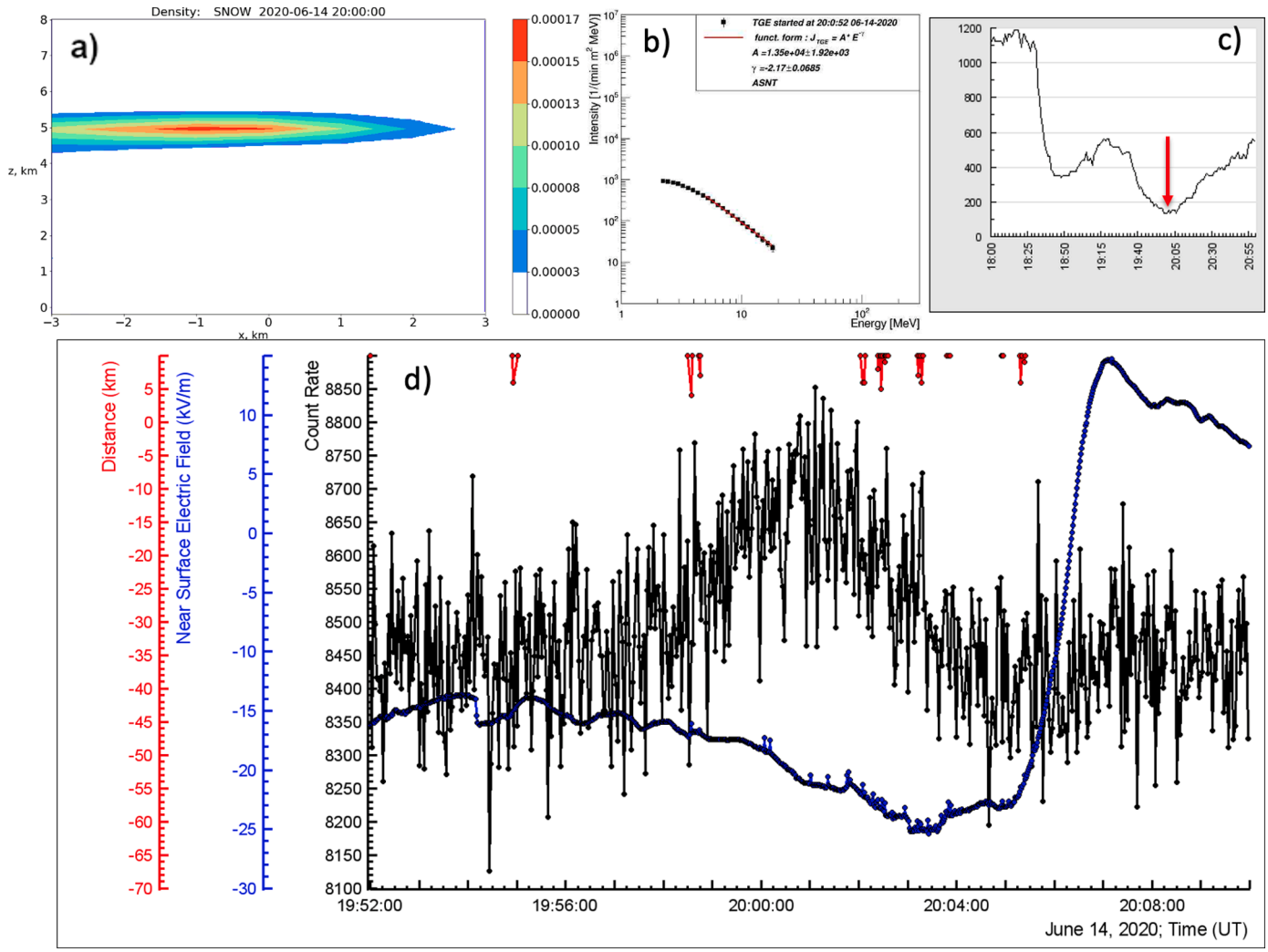

Fig. 10. a) 2-dimensional pattern of the hydrometeor density (kg/m3), according to the simulation using WRF, b) Energy spectra of the gamma rays; c0 distance to the cloud base; c) zoomed version of third TGE (the notion is the same as in Fig. 7).

Both measured parameters of particle fluxes and hydrometeors density maps obtained using the WRF model give a consistent explanation of the atmospheric electric structures supported by 3 TGEs that occurred on 14 June 2020.

Declaration of Competing Interest

The authors declare no conflict of interest.

Acknowledgement

We thank the staff of the Aragats Space Environmental Center for the operation of particle detectors on Mount Aragats. A. C. thanks S. Soghomonyan for the valuable comments and for the useful, multi-year discussions on the origin of the atmospheric electric field. The data for this study in graphical and numerical forms are available by the multivariate visualization software platform ADEI on the WEB page of the Cosmic Ray Division (CRD) of the Yerevan Physics Institute, http://adei.crd.yerphi.am/adei. In the WIKI section explanations of facilities and how to select necessary data are posted. The authors thank S. Chilingaryan for his continuous efforts to maintain and improve Web-based data analysis facilities for a large stream of data coming online from the Mount Aragats research station.

References

[1] S. Agostinelly, J. Allison, A. Amako, et al., Geant4—A simulation toolkit, NIM 506 (2003) 250.
[2] L.P. Babich, I.M. Kutsyk, E.N. Donskoy, et al., Comparison of relativistic runaway electron avalanche rates obtained from Monte Carlo simulations and kinetic equation solution, IEEE Trans. Plasma Sci. 29 (3) (2001) 430–438. https://doi.org/10.1109/27.928940.
[3] S. Buitink, H. Falcke, et al., Monte Carlo simulations of air showers in atmospheric electric fields, Astropart. Phys. 33 (2010) 1.
[4] A. Chilingarian, Development of the Data Processing Methods in High Energy Physics. From a Data Base to a Knowledge Base, Preprint YerPhi-1327 (22) (1991).
[5] A. Chilingarian, B. Mailyan, L. Vanyan, Recovering of the energy spectra of electrons and gamma rays coming from the thunderclouds, Atmos. Res. 1 (2012) 114–115.
[6] A. Chilingarian, H. Mkrtchyan, Role of the Lower Positive Charge Region (LPCR) in initiation of the Thunderstorm Ground Enhancements (TGEs), Phys. Rev. D 86 (2012), 072003.
[7] A. Chilingarian, T. Karapetan, L. Melkumyan, Statistical analysis of the Thunderstorm Ground Enhancements (TGEs) detected on Mt, Aragats. J. Adv. Space Res. 52 (2013) 1178.
[8] A Chilingarian, G. Hovsepyan, B. Mailyan, In situ measurements of the Runaway Breakdown (RB) on Aragats mountain, Nuclear Inst. Methods Phys. Res. A 874 (2017) 19–27.
[9] A. Chilingarian, H. Mkrtchyan, G. Karapetyan, B. Sargsyan, A. Arestakesyan, Catalog of 2017 thunder- storm ground enhancement (TGE) events observed on Aragats, Sci. Rep. 9 (2019) 6253.
[10] A. Chilingarian, G. Hovsepyan, A. Elbekian, T. Karapetyan, L. Kozliner, H. Martoian, B. Sargsyan, Origin of enhanced gamma radiation in thunderclouds, Phys. Rev. Res. 1 (2019), 033167.
[11] A. Chilingarian, Y. Khanikyants, V.A. Rakov, S. Soghomonyan, Termination of thunderstorm-related bursts of energetic radiation and particles by inverted-

polarity intracloud and hybrid lightning discharge, Atmos. Res. 233 (104713) (2020).
[12] A. Chilingarian, T. Karapetyan, H. Hovsepyan, Maximum strength of the atmospheric electric field, Phys. Rev. D 103 (2021), 043021.
[13] A. Chilingarian, G. Hovsepyan, B. Sargsyan, Circulation of Radon progeny in the terrestrial atmosphere during thunderstorms, Geophys. Res. Lett. 47 (2020), e2020GL091155, https://doi.org/10.1029/2020GL091155.
[14] A. Chilingarian, G. Hovsepyan, T. Karapetyan, et al., Structure of thunderstorm ground enhancements, PRD 101 (2020), 122004.
[15] A. Chilingarian, Y. Khanikyants, V.A. Rakov, S. Soghomonyan, Termination of thunderstorm-related bursts of energetic radiation and particles by inverted-polarity intracloud and hybrid lightning discharge, Atmos. Res. 233 (104713) (2020).
[16] J.R. Dwyer, A fundamental limit on electric fields in air, Geophys. Res. Lett. 30 (20) (2003) 2055. https://doi.org/10.1029/2003GL017781.
[17] G.J. Fishman, P.N. Bhat, v Mallozzi, et al., Discovery of intense gamma ray flashes of atmospheric origin, Science 264 (1994) 1313.
[18] A.V. Gurevich, G. Milikh, R. Roussel-Dupre, Runaway electron mechanism of air breakdown and preconditioning during a thunderstorm, Phys. Lett. A 165 (1992) 463.
[19] D. Heck, J. Knapp, J.N. Capdevielle, G. Schatz, and T. Thouw, Report No. FZKA 6019, 1998, Forschungszentrum, Karlsruhe, https://www.ikp.kit.edu/corsika/70.php.
[20] G. Hovsepyan, An Automatic Algorithm for the recovering of TGE differential energy spectra, in: Proceeding of TEPA-2018 conference, Armenia, Tigran Mec, 2018, p. 97. Nor-Amberd.
[21] J. Kuettner, The electrical and meteorological conditions inside thunderclouds, J. Meteorol. 7 (1950) 322.
[22] T.C. Marshall, M.P. McCarthy, W.D. Rust, Electric field magnitudes and lightning initiation in thunderstorms, J. Geophys. Res. 100 (1995) 7097.
[23] T. Sato, Analytical Model for Estimating the Zenith Angle Dependence of Terrestrial Cosmic Ray Fluxes, PLoS ONE 11 (8) (2018), e0160390. http://phits.jaea.go.jp/expacs/.
[24] M. Stolzenburg, T.C. Marshall, W.D. Rust, E. Bruning, D.R. MacGorman, T. Hamlin, Electric field values observed near lightning flash initiations, Geophys. Res. Lett. 34 (2007) L04804.
[25] E.K. Svechnikova, N.V. Ilin, E.A. Mareev, Recovery of electrical structure of the cloud with use of ground-based measurement results, in: Proceeding of TEPA-2018 conference, Armenia, Tigran Mec, 2018, p. 75. Nor-Amberd.
[26] E.K. Svechnikova, N.V. Ilin, E.A. Mareev, et al., Characteristic features of the clouds producing thunderstorm ground enhancements, JGR Atmosphere (2021), https://doi.org/10.1029/2019JD030895.
[27] H. Tsuchiya, et al., Long-duration gamma ray emissions from 2007 to 2008 winter thunderstorms, J. Geophys. Res. 116 (2011) D09113, https://doi.org/10.1029/2010JD015161.
[28] Y. Wada, T. Enoto, M. Kubo et al., Meteorological aspects of gamma-ray glows in winter thunderstorms, GRL 48, p. e2020GL091910, doi.org/10.1029/2020GL091910.